

A decentralized HC-ADMM approach for large antenna arrays

Jyothi B. R.¹, Manjanaik Naganaik²

¹Department of Electronics and Communication Engineering, K. L. S Gogte Institute of Technology, Affiliated to Visvesvaraya Technological University, Belagavi, India

²Department of Electronics and Communication Engineering, University Brahmappa Devendrappa Tavanappanavar College of Engineering, Affiliated to Visvesvaraya Technological University, Belagavi, India

Article Info

Article history:

Received Dec 18, 2023

Revised Jan 19, 2024

Accepted Feb 16, 2024

Keywords:

ADMM

Data transfer

Radio frequency chain

Spectral efficiency

Transceiver

ABSTRACT

This work addresses the evolving landscape of internet of things (IoT) applications and large antenna array systems, where optimizing spectral efficiency and simplifying design complexities are crucial. Focusing on two key challenges, the study introduces a novel hybrid analog-digital transceiver strategy tailored for frequency-selective channels. By integrating Shannon and Hartley theorems, the approach enhances data transfer rates, thereby optimizing radio frequency (RF) chain utilization in large-scale antennas. To achieve a balance between transceiver performance and hardware complexity, the study employs a decentralized alternating direction method of multipliers (ADMM) framework. The proposed hybrid consensus ADMM algorithm (HC-ADMM) ensures efficient convergence in decentralized optimization scenarios. Comparative analyses with ADMM and existing system transceiver optimization (ESTO) models highlight HC-ADMM's superior performance across key metrics such as spectral efficiency, efficiency per cell, total efficiency, and optimal scheduling of user equipment (UEs). Particularly notable is HC-ADMM's advanced optimization capabilities as the number of transmit antennas increases, positioning it as a promising approach for enhancing overall communication network performance.

This is an open access article under the [CC BY-SA](https://creativecommons.org/licenses/by-sa/4.0/) license.



Corresponding Author:

Jyothi B. R.

Department of Electronics and Communication Engineering, K. L. S Gogte Institute of Technology

Affiliated to Visvesvaraya Technological University

Belagavi-590018, India

Email: jyothiresearch2024@gmail.com

1. INTRODUCTION

Establishing reliable and efficient internet of things (IoT) networks is paramount to accommodate the ever-growing multitude of IoT devices and the seamless transmission of voluminous data. Among the various smart applications, wireless communication and data aggregation stand out as extensively applied IoT functions for swift and dependable data transfer [1]-[3]. In this context, IoT employs distributed sensors that connect to a central source, facilitating the simultaneous transmission of aggregated data to a fusion center. The fusion center, leveraging the received information, endeavors to retrieve the data in a unified format. This approach to joint data transmission significantly enhances performance in diverse IoT applications, including object recognition, target tracking, and real-time network monitoring [4], [5]. IoT systems typically feature small sensors and actuators, each equipped with a single antenna. Nevertheless, IoT networks can expand significantly in size, necessitating the incorporation of numerous multi-antenna arrays and radio frequency (RF) chains, contingent upon the specific application requirements [6]-[8]. Supplying adequate energy to power all these sensors, arrays, and RF chains within energy-constrained IoT

applications can pose challenges. Furthermore, the use of compact-sized sensors can lead to a dearth of available frequency spectrum resources, thereby driving the need to adopt higher frequency bands such as millimeter Wave (mmWave) [9], [10]. This research investigates a standard multi-antenna-based IoT system designed to facilitate rapid data transfer, consequently delivering high spatial multiplexing gains and diversity [11]. Although the deployment of multiple-input multiple-output (MIMO) systems in IoT scenarios can enhance spectral efficiency, reduce computational complexity, and improve cost-effectiveness, it is often executed through full digital beamforming techniques [12], [13]. Full-digital beamforming inherently involves a one-to-one correspondence between the number of RF chains and antennas, which can be both cost-intensive and energy-draining in transceiver setups. Consequently, the adoption of traditional full-digital beamforming techniques may augment design complexity, resulting in amplified power losses, particularly within large antenna arrays. Analog and linear beamforming techniques, although less complex and more energy-efficient than their digital counterparts, tend to exhibit lower spectral efficiency and spatial gain [14]. To mitigate the limitations inherent in analog and digital beamforming techniques, researchers have explored the concept of hybrid beamforming techniques [15], [16].

This study primarily delves into the realm of beamforming design within mmWave SU-MIMO systems, where both the transmitter and receiver harness large-scale antenna arrays with a hybrid beamforming structure. In such configurations, it is observed that with a sufficiently large number of antennas, the covariance matrices of the channel at different subcarriers share approximately the same set of eigenvectors, attributed to the sparsity of mmWave channels. This observation suggests that optimal fully-digital eigen-beam formers at all subcarriers are approximately the same. The primary aim of incorporating hybrid beamforming techniques is to minimize the number of RF chains in extensive antenna setups. The hybrid beamforming technique comprises two core components: analog and digital. The analog element manipulates various stages of RF signals using cost-effective phase shifters, while the digital component remains conventional. The reduced reliance on RF chains results in significant reductions in hardware costs. Nonetheless, the complexity introduced by coupled variables and intricate phase shifters makes the operation of hybrid transceivers more challenging. Existing research often resorts to an alternating direction method of multipliers (ADMM) framework for designing hybrid transceivers. In IoT applications, full-digital transceiver designs are prevalent, but their dependence on correlation exacerbates operational complexity, rendering them less suitable for cost-effective IoT applications.

This research endeavors to implement a hybrid transceiver design tailored for IoT applications, striving to offer the best of both worlds. The key contributions of this research are as follows: The paper explores an IoT network wherein both sensors and fusion centers are equipped with hybrid analog and digital components, delivering full digital performance without amplifying complexity and hardware expenses. This paper attempts to deploy a hybrid transceiver design for IoT application. The main contributions of this paper are as follows: This paper considers an IoT network wherein both the sensors and fusion centers are equipped with hybrid analog and digital components which provides complete digital performance without increasing the complexity and hardware cost which is looks like a general structure as shown in the Figure 1. For analog components, the optimization problem is considered to be a non-convex problem because of the unit modulus. In this research, a decentralized consensus ADMM is implemented in order to achieve a balanced tradeoff between the performance and complexity. In the ADMM framework, the actual problem is segmented into multiple small problems and for each sub problem the solution is obtained in the closed form. Results of the simulation analysis show that the performance of ADMM based approach is better than the full digital solutions. This research states that the research related to energy consumption improvement for hybrid transceivers is currently under development and includes the extension of the proposed approach to partially connected hybrid solutions and frequency selective channels.

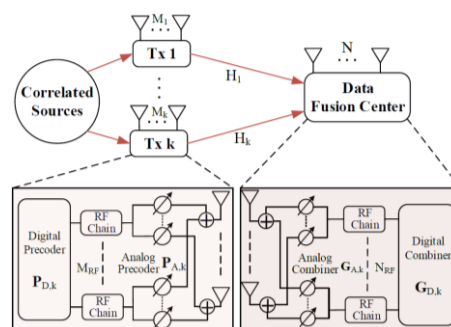


Figure 1. A system model of wireless sensor network with analog digital hybrid transceivers [17]

The rest of the paper is organized as follows: Section 2 reviews existing techniques related to the recommended study. In section 3 discusses the methodology involved in this research including the design of analog-digital hybrid transceiver model and ADMM framework. Section 4 presents the results of the simulation analysis and section 5 concludes the paper with experimental observations and future scope.

2. LITERATURE SURVEY

Several existing literary works have also deployed the design of hybrid transceivers and several algorithms have been implemented for addressing the problem associated with it Tsinos *et al.* [18], Zhang *et al.* [19], Zhao *et al.* [20]. For instance, the orthogonal matching pursuit (OMP) algorithm is one of the extensively used techniques in the design of hybrid transceiver and mmWave communication systems Darabi *et al.* [21]. The OMP algorithm was used to design a hybrid beamforming (BF) technique wherein the analog BF was designed at the transmitter and the digital BF was deployed at the receiver in order to increase the sum rate. Results of the simulation analysis show that the OMP algorithm reduced the hardware complexity and the OMP based hybrid BF outperforms other techniques when deployed for mmWave communications. This approach also reduced the number of RF chains. A codebook based design for hybrid transceiver is proposed in He *et al.* [22], Shaban *et al.* [23] which minimizes the complexity of transceiver design in mmWave channels. The effectiveness of this approach mainly relies on the structure of the codebook and the performance deteriorates when the measured channel state information (CSI) is not accurate. In recent times, various near-optimal algorithms were introduced to simplify the design problems in analog transceivers such as matrix decomposition Ni *et al.* [24], Zhu *et al.* [25].

Based on the optimization ideas, analog or digital precoders were implemented in Qiao *et al.* [26]. These algorithms aim to minimize the euclidean distance between the optimal and hybrid precoder. To reduce the computational complexity, this research employs a ADMM based alternative optimization algorithm wherein the number of transmitting antennas is higher than the receiving antennas and when the amount of data streams is small. Considering the effectiveness of optimization algorithms, alternating optimization (AO) techniques are implemented for analog and digital precoders as mentioned in Liu *et al.* [27]. The AO algorithm is used to approximate the optimal solution for full digital systems. For analog precoder systems, the iterative algorithm is implemented to optimize the objective function. Another algorithm for optimization known as matrix monotonic optimization is proposed for designing hybrid transceivers in Xing *et al.* [28] which can be applied to different applications. The matrix optimization can be applied for both linear and nonlinear transceivers for achieving better performance. The work proposed in Tsinos *et al.* [29] employed an ADMM-based hybrid transceiver design which increases the spectral efficiency in wireless mmWave systems. In particular, a projected gradient descent (PGD) method is implemented along with phase projection for addressing the problem associated with energy consumption and hardware complexity. These algorithms intend to design hybrid transceivers simultaneously.

Tsinos and Ottersten [30] proposed an ADMM technique for designing an analog beamforming technique in wireless communication systems. In most of the IoT applications, a fully digital transceiver design is employed for effective communication. For example, a physical layer based reliable beamforming technique for IoT systems is proposed in Huang *et al.* [31], Guo *et al.* [32], Xiao *et al.* [33]. Several research works have also focused on the implementation of hybrid beamforming in IoT networks. In particular, a semidefinite programming relaxation (SDR) based hybrid beamforming technique is proposed in Yang *et al.* [34]. The SDR based approach is implemented to minimize the complexity of the hybrid beamforming technique. The digital BF technique and the analog BF technique is employed for addressing the complexity issues. The AO algorithm along with SDR technique effectively solve the problems associated with beamforming. Results of the simulation analysis show that the proposed approach appropriately balances the SINR of all users. It can be inferred from the existing works, that deploying optimization algorithms have a significant impact in reducing the hardware complexity and improving the spectral efficiency of the large-scale antenna systems.

3. METHOD

3.1. System model

This research intends to enhance spectral efficiency of the hybrid analog-digital transceiver and reduce the Bit error rate (BER) using a decentralized consensus ADMM algorithm. This research presents an innovative approach for optimizing the utilization of RF chains in large-scale antenna systems through the incorporation of analog-digital hybrid transceiver technique specifically tailored for frequency-selective channels in the context of a hybrid IoT communication system. The system under consideration comprises spatially distributed IoT sensors collaborating with a fusion center (FC) in monitoring and targeting a spatially correlated physical process. The communication system involves K IoT sensor, each equipped with

N antennas, which collectively monitor the network environment and transmit signals denoted as (Tx_k) where $x_k \in \mathbb{C}^{N_s \times 1}$ represents the transmitted signal from the k^{th} sensor. The correlation matrix x is defined as $x = [x_1^T, x_2^T, \dots, x_K^T]$, and its expectation, denoted as Rx , is formulated as per (1), highlighting the correlated nature of the transmitted signals.

$$Rx = E \{ [x_1^T, x_2^T, \dots, x_K^T]^T [x_1^T, x_2^T, \dots, x_K^T]^* \} \quad (1)$$

The transmission path between the FC and the transmitters (Tx_k) is represented by $H_k \in \mathbb{C}^{N \times M_k}$ where N and M_k denote the number of antennas in the FC and k^{th} transmitter, respectively. To facilitate efficient data transmission across multiple channels, the paper proposes the implementation of different RF chains, namely, number of radio frequency (NRF) and multiple radio frequency (MRF), near the IoT sensors and FC. This design choice, with the number of RF chains being less than the number of antennas, enhances system simplicity and significantly reduces energy consumption in the antenna arrays. The schematic of the proposed system model is shown in Figure 2.

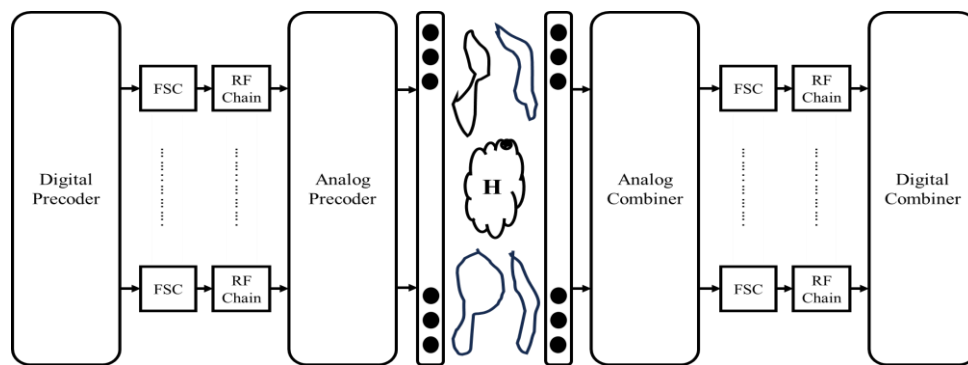


Figure 2. System model for hybrid beamforming

The system model, depicted in Figure 2 as a schematic for hybrid beamforming, illustrates the integration of the proposed hybrid transceiver techniques for optimizing RF chain utilization in large-scale antennas. The study assumes uniform generalization ability among all transmitters, each equipped with an equal number of antennas. Furthermore, it is assumed that IoT sensors transmit signals through orthogonal channels, employing time and frequency division multiple access, expressed as $y = [y_1^T, y_2^T, \dots, y_K^T] \in \mathbb{C}^{N_{RF} \times 1}$. The noise vector's correlation matrix, denoted as R_N , is defined in (2).

$$R_N = \text{diag} \{ R_{n1}, R_{n2}, \dots, R_{nk} \} \quad (2)$$

Here, R_{nk} represents the correlation matrix, and nk denotes the noise vector. The proposed model aims to optimize the utilization of RF chains in large-scale antennas by leveraging analog-digital hybrid transceiver techniques tailored for the challenges posed by frequency-selective channels in the context of a hybrid IoT communication system.

3.2. Shannon theorem and hartley theorem

This study proposes an innovative approach to optimize the utilization of RF chains in large-scale antenna systems by integrating analog-digital hybrid transceiver techniques tailored for frequency-selective channels. In the context of a multi-input, multi-output (MIMO) system, the Shannon-Hartley theorem is recognized for its comprehensive analysis, providing a threshold limit for transmitting information in frequency-bounded channels. This limit, known as the Shannon-Hartley limit, is traditionally applied to systems with a reduced number of antennas for each transceiver. However, this paper explores the potential for exceeding the Shannon-Hartley limit by increasing the data rate in multi-antenna transceivers. The Shannon-Hartley theorem establishes a maximum data rate (MDR) constraint for transmitting data over a Gaussian channel, considering the signal-to-noise ratio (SNR) and power factors. The theorem is mathematically expressed as in (3).

$$I(S; S + T) \leq \left[\left(\frac{1}{2} \right) \log \left(1 + \left(\frac{\tau^2}{\sigma^2} \right) \right) \right] \quad (3)$$

Where $I(S; T) = h(S) - h(S|T)$ represents the mutual information between S and T mutually, the term $h(S) = -\int sf(s) \log f(s) dx$ denotes the differential entropy of the random variable S , with f representing the probability density function (PDF). This theorem sets the theoretical limit for the data transfer rate, considering the SNR and noise in the transmission channel. In conclusion, this proposed model leverages analog-digital hybrid transceiver techniques to optimize RF chain utilization in large-scale antennas. The study explores the potential to surpass the Shannon-Hartley limit by employing advanced transceiver configurations specifically designed for frequency-selective channels. By integrating these techniques, the system aims to enhance data transmission efficiency, allowing for increased data rates beyond the traditional limits imposed by the Shannon-Hartley theorem. This novel approach contributes to the ongoing efforts to optimize communication systems, particularly in scenarios involving large-scale antenna deployments and frequency-selective channel conditions.

3.3. Decentralized ADMM consensus method

In this work, the decentralized optimization problem is addressed through the utilization of the ADMM, presenting an effective model and algorithm. ADMM is a powerful optimization technique suitable for decentralized systems where collaboration among nodes is essential. In this context, the algorithm orchestrates the exchange of information among decentralized nodes, facilitating the convergence towards a consensus solution. The decentralized ADMM framework leverages the principle of decomposing the original problem into subproblems, each handled by individual nodes, while a consensus mechanism ensures coherence in the overall solution. The ADMM algorithm acts as a bridge between decentralized nodes, allowing them to collectively optimize a global objective function while preserving local autonomy. It provides a balance between communication efficiency and computational complexity by dividing the optimization task into manageable components. This approach minimizes the need for extensive information exchange while still achieving a consensus solution.

The proposed Hybrid Consensus ADMM approach takes this decentralized optimization further by introducing a hybrid strategy. This strategy likely involves integrating additional components or a mechanism to enhance the performance of the ADMM in specific scenarios. The hybridization is aimed at addressing challenges related to hardware complexity, by introducing adaptive parameter and novel technique which optimizes the trade-off between transceiver performance and hardware resources. The goal is to design a decentralized optimization scheme that not only converges efficiently but also considers practical constraints associated with hardware capabilities, leading to a more balanced and practical solution for decentralized communication systems. Hence to achieve this, consider a decentralized optimization problem with nodes represented by indices (nodes) i and j . Let f_i denote the local cost function available to node. The penalty factor is denoted by ρ and x_i^{k+1} , y_i^{k+1} , and z_i^{k+1} represent the updated values at iteration $k + 1$ for ADMM, D-ADMM, and FC-ADMM, respectively. The initial updates are x^0 , y^0 , and z^0 , and \mathcal{N}_i represents the set of neighboring nodes for node i . Additionally, E_{jj} represents the updated packets by the FC, and D_{ii} represents the total number of packets. The ADMM update for node i is done using Equation (4). The dual variable update for node y_i is done using (5). The FC updates the decision by averaging local copies and broadcasts the updated value z_j^{k+1} back to all nodes using (6).

$$x_i^{k+1} = (\nabla f_i + \rho |\mathcal{N}_i| I)^{-1} \left[\frac{\rho}{2} \sum_{j \in \mathcal{N}_i} (x_i^k + x_j^k) - y_i^k \right] \tag{4}$$

$$y_i^{k+1} = y_i^k + \frac{\rho}{2} \sum_{j \in \mathcal{N}_i} (x_i^{k+1} + x_j^{k+1}) \tag{5}$$

$$z_j^{k+1} = \frac{1}{E_{jj}} \sum_{i \in \mathcal{N}_i} x_i^{k+1} \tag{6}$$

Further, the consensus ADMM algorithm is presented as in Algorithm 1.

Algorithm 1. Hybrid consensus ADMM algorithm (HC-ADMM)

```

Start
Input  $\rho, x^0, z^0, y^0 = 0$ 
Step 1 While Stopping criterion not satisfied
Step 2 For each node  $i = 1, \dots, N$ :
Update  $x_i^{k+1}$  by solving  $\nabla f_i(x_i^{k+1}) + \rho |\mathcal{N}_i| x_i^{k+1} = \rho \sum_{j \in \mathcal{N}_i} (z_j^k - y_i^k)$ ;
Send  $x_i^{k+1}$  to all incident FCs and neighbors
End For

Step 3 For each FC  $j = 1, \dots, M$ :
Update  $z_j^{k+1}$  by solving  $z_j^{k+1} = \frac{1}{E_{jj}} \sum_{i \in \mathcal{N}_i} x_i^{k+1}$ 
    
```

```

Send  $z_j^{k+1}$  to all incident nodes
End For

Step 4 For each node  $i = 1, \dots, N$ :
Update  $y_i^{k+1}$  by solving  $y_i^{k+1} = y_i^k + \rho(D_{ii}x_i^{k+1} - \sum_{j \in \mathcal{N}_i} z_j^{k+1})$ 
End for
Stop

```

The hybrid consensus ADMM algorithm begins by initializing the input parameters, including the penalty factor (ρ), initial values for variables (x^0, z^0, y^0), and setting the iteration counter to zero. The algorithm iteratively executes the following steps until a stopping criterion is met. In Step 2, for each node i in the network ($i = 1, \dots, N$), the algorithm updates the variable x_i^{k+1} by solving a convex optimization problem. This problem involves the gradient of the local cost function (∇f_i) and a regularization term ($\rho|\mathcal{N}_i|x_i^{k+1}$), with constraints driven by the consensus term $\rho \sum_{j \in \mathcal{N}_i} (z_j^k - y_i^k)$. The updated variable x_i^{k+1} is then broadcasted to all incident fusion centers (FCs) and neighboring nodes. In step 3, for each FC j in the network ($j = 1, \dots, M$), the algorithm updates the variable z_j^{k+1} by averaging the received values from neighboring nodes ($\sum_{i \in \mathcal{N}_i} x_i^{k+1}$) and scaling by the inverse of the updated packets ($\frac{1}{E_{jj}}$). The updated z_j^{k+1} is then sent to all incident nodes. In step 4, for each node i in the network ($i = 1, \dots, N$), the algorithm updates the dual variable y_i^{k+1} based on the received information. This update involves a combination of the previous dual variable (y_i^k), a term related to the total number of packets ($D_{ii}x_i^{k+1}$), and the consensus term from neighboring FCs ($\sum_{j \in \mathcal{N}_i} z_j^{k+1}$). The algorithm repeats these steps until a predefined stopping criterion is satisfied, indicating convergence. The stopping criterion can be defined based on the convergence of the variables or other relevant metrics, ensuring that the algorithm iterates until a satisfactory consensus solution is reached. The HC-ADMM algorithm facilitates decentralized optimization by enabling information exchange among nodes and fusion centers, promoting consensus in the iterative process. The results achieved by the HC-ADMM is discussed in the next section.

4. RESULTS AND DISCUSSION

4.1. System requirement

To run the HC-ADMM, conventional ADMM, and existing system transceiver optimization (ESTO) method [35], Windows 11 operating system was considered. A minimum of 8 GB RAM is necessary to ensure smooth execution of the optimization algorithms. Additionally, MATLAB was preferred platform for implementing these methods, so it is essential to have MATLAB installed on the system. These specifications provide the computational resources and software environment needed to effectively carry out the optimization processes and evaluate the performance of the transceiver systems.

4.2. Evaluation parameters

In this work, initially, random values are generated to evaluate antenna parameters. These parameters include the path loss exponent, the number of directions to look for interfering cells, and the percentage of the radius inside the cell where no user equipment (UEs) is allowed. The parameter considered for evaluation are presented in Table 1.

Table 1. Parameters considered for evaluation

Parameters	Values
Number of nodes	10
Number of users	10
Path loss exponent	1.8%
Radius inside the cell	0.05
Number of random users	500000

In the context of this work, the Monte-Carlo simulations for antenna system evaluation, key parameters are established. Each cell is assigned a specific number of random users, contributing to the stochastic nature of the simulation. The range for each base station antenna is defined, and the distribution of antennas follows a logarithmic scale, ensuring a balanced deployment. For evaluation of this work the following metrics are used.

Spectral Efficiency represents how efficiently the available bandwidth is utilized to transmit data. It is expressed as the ratio of the net data rate to the channel bandwidth. Higher spectral efficiency indicates a more effective utilization of the available spectrum for transmitting data, a crucial metric in assessing the performance of communication systems, especially in bandwidth-limited scenarios. The effective rate at which data is transmitted over the communication channel, typically measured in bits per second (bps). The range of frequencies allocated for the communication channel, measured in hertz (Hz). In the (7) is used for evaluating the spectral efficiency.

$$Spectral\ Efficiency = \frac{Net\ Data\ Rate(bps)}{Channel\ Bandwidth\ (Hz)} \tag{7}$$

4.3. Results

In the analysis of base station tower performance, a comparison of three models HC-ADMM, ADMM, and ESTO was conducted, focusing on spectral efficiency concerning the number of transmit antennas. Figure 3 visually demonstrates the superiority of the HC-ADMM model in terms of spectral efficiency. The graph illustrates that as the number of transmit antennas increases, the spectral efficiency achieved by HC-ADMM surpasses that of both ADMM and ESTO methods. This result signifies the enhanced efficiency and optimization capabilities of the HC-ADMM approach in comparison to conventional ADMM and the ESTO method. The graphical representation in Figure 3 provides a clear and compelling visualization of the performance advantages of the HC-ADMM model in optimizing spectral efficiency in the context of increasing transmit antennas. In the evaluation of spectral efficiency per cell, a comparative study among three models HC-ADMM, ADMM, and ESTO was conducted. Figure 4 visually presents the results, showcasing the spectral efficiency achieved per cell concerning the number of base station antennas. The graph distinctly illustrates that, as the number of base station antennas increases, the spectral efficiency per cell for the HC-ADMM model surpasses that of both the ADMM and ESTO methods. This outcome signifies the superior optimization capabilities of the HC-ADMM approach compared to conventional ADMM and the ESTO method. The graphical representation in Figure 4 provides a comprehensive and intuitive view, emphasizing the efficiency gains offered by the HC-ADMM model in optimizing spectral efficiency per cell in comparison to alternative approaches.

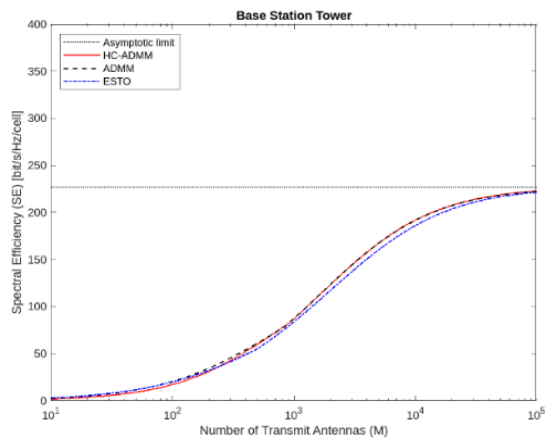


Figure 3. Base station tower

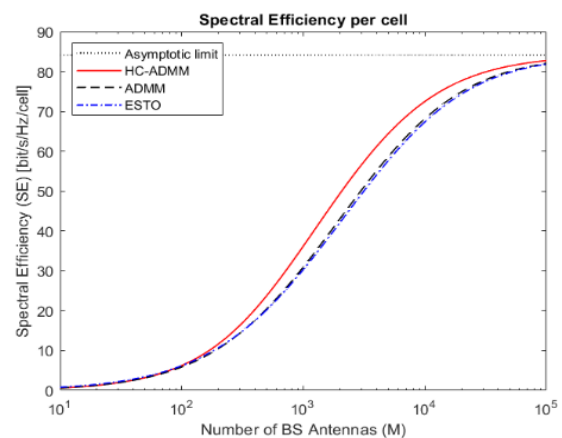


Figure 4. Spectral efficiency per cell

In the assessment of total efficiency, a comparative analysis was conducted among three models: HC-ADMM, ADMM, and ESTO. The graphical representation in Figure 5 highlights the spectral efficiency concerning the number of transmit antennas for each model. The graph clearly demonstrates that, with an increasing number of transmit antennas, the total efficiency achieved by the HC-ADMM model outperforms both the ADMM and ESTO methods. This result underscores the superior optimization capabilities of the HC-ADMM compared to conventional ADMM and the ESTO method. The visual representation in Figure 5 provides a compelling insight into the efficiency gains offered by the HC-ADMM model, establishing its efficacy in optimizing Spectral Efficiency in comparison to alternative methods. In the evaluation of UE antennas, a comparative study was conducted involving three models: HC-ADMM, ADMM, and ESTO.

Figure 6 visually represents the results, specifically focusing on the optimal number of scheduled UE concerning the number of base station antennas. The graph vividly illustrates that, with an increasing

number of base station antennas, the HC-ADMM model achieves a superior optimal number of scheduled UEs when compared to both the ADMM and ESTO methods. This outcome underscores the advanced optimization capabilities of the HC-ADMM in contrast to conventional ADMM and the ESTO method. Figure 6 provides a clear visual representation, emphasizing the efficiency gains offered by the HC-ADMM model in determining the optimal number of scheduled UEs when compared to alternative approaches. In the assessment of the number of users, a comprehensive comparison was conducted among three models: HC-ADMM, ADMM, and ESTO.

The graphical representation in Figure 7 highlights the results, specifically focusing on the optimal number of scheduled UEs concerning the number of base station (BS) antennas. The graph compellingly illustrates that, as the number of BS antennas increases, the HC-ADMM model outperforms both the ADMM and ESTO methods in achieving a superior optimal number of scheduled UEs. This finding underscores the advanced optimization capabilities of the HC-ADMM concerning the determination of the optimal number of scheduled UEs when compared to conventional ADMM and the ESTO method. The visual representation in Figure 7 provides a clear and insightful view, emphasizing the efficiency gains offered by the HC-ADMM model in optimizing the number of users in comparison to alternative approaches.

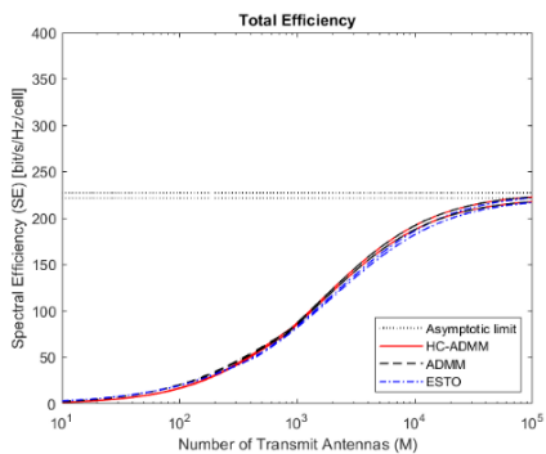


Figure 5. Total efficiency

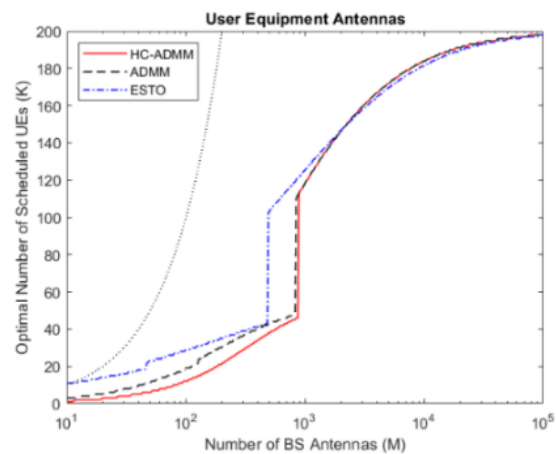


Figure 6. UE antennas

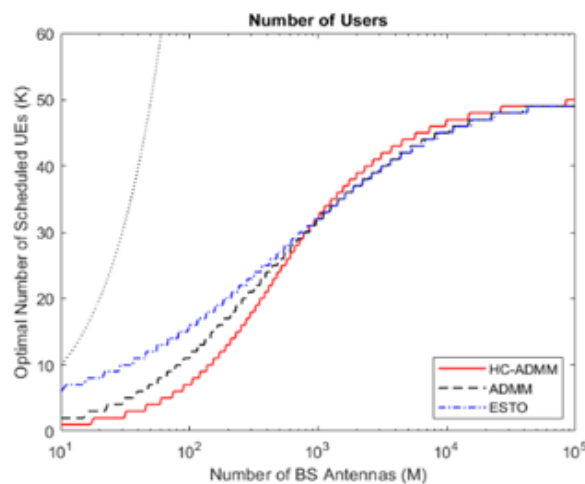


Figure 7. Number of users

4.4. Discussion

The results obtained from the comparative analysis of the HC-ADMM, ADMM, and ESTO models provide valuable insights into their respective performances in optimizing various aspects of base station tower operations. The focus on spectral efficiency, spectral efficiency per cell, total efficiency, and the

optimal number of scheduled UEs and users sheds light on the efficacy of each model in different scenarios. Figure 3 demonstrates that as the number of transmit antennas increases, the HC-ADMM model consistently outperforms both the ADMM and ESTO methods in achieving higher spectral efficiency. This indicates that the HC-ADMM is more effective in utilizing available resources, optimizing the spectral efficiency in comparison to conventional ADMM and the ESTO method. In Figure 4, the superior performance of the HC-ADMM model is again evident as the spectral efficiency per cell increases with a growing number of base station antennas. This reinforces the notion that HC-ADMM excels in optimizing spectral efficiency on a per-cell basis, showcasing its advanced optimization capabilities compared to ADMM and ESTO. The analysis of total efficiency, as depicted in Figure 5, solidifies the superiority of the HC-ADMM model. With an increasing number of transmit antennas, the total efficiency achieved by HC-ADMM surpasses that of ADMM and ESTO. This underlines the comprehensive optimization capabilities of HC-ADMM in maximizing overall efficiency in comparison to alternative methods. Examining Figure 6, the HC-ADMM model stands out in determining the optimal number of scheduled UEs concerning the number of base station antennas. The graph visually conveys the efficiency gains offered by HC-ADMM in optimizing the scheduling of UEs, highlighting its superiority over ADMM and ESTO. Finally, in Figure 7, the analysis of the number of users further accentuates the advanced optimization capabilities of HC-ADMM. As the number of BS antennas increases, the HC-ADMM model consistently achieves a superior optimal number of scheduled UEs compared to ADMM and ESTO. This underscores HC-ADMM's effectiveness in optimizing the number of users in the system. The consistent superior performance of the HC-ADMM model across various metrics underscores its efficacy in optimizing base station tower operations. The advanced optimization capabilities of HC-ADMM, particularly in spectral efficiency, efficiency per cell, total efficiency, and user scheduling, make it a promising approach for enhancing the overall performance of communication networks. These findings provide valuable guidance for future implementations and optimizations in the field of wireless communication systems. The Table 2. summarizes the comparative performance of the three models across different metrics. The "Higher" and "Lower" indications emphasize the superior performance of the HC-ADMM model in each aspect considered.

Table 2. Comparative study

Metric	HC-ADMM	ADMM	ESTO
Spectral efficiency	Higher	Lower	Lower
Spectral efficiency per cell	Higher	Lower	Lower
Total efficiency	Higher	Lower	Lower
Optimal scheduled UEs	Higher	Lower	Lower
Optimal number of users	Higher	Lower	Lower

5. CONCLUSION

In the rapidly evolving landscape of IoT applications and large antenna array systems, the integration of hybrid analog-digital transceivers is proving to be a pivotal strategy for optimizing spectral efficiency and simplifying design complexities. This study addresses two paramount challenges in this domain, presenting innovative solutions to enhance the performance of large-scale antennas. The first challenge tackled involves the optimization of RF chain utilization through tailored analog-digital hybrid transceiver techniques, specifically designed for frequency-selective channels. Leveraging Shannon and Hartley theorems, the approach enhances data transfer rates, contributing to improved spectral efficiency. The second challenge is addressed through the implementation of a ADMM framework, providing a balance between transceiver performance and hardware complexity. The proposed HC-ADMM stands out, ensuring efficient convergence in decentralized optimization scenarios. The comparative analysis of HC-ADMM, ADMM, and ESTO models provides a comprehensive understanding of their respective performances in optimizing various facets of base station tower operations. The emphasis on spectral efficiency, spectral efficiency per cell, total efficiency, and optimal scheduling of UEs and users sheds light on the models' efficacy across diverse scenarios. The results consistently highlight the superior performance of the HC-ADMM model. As the number of transmit antennas increases, HC-ADMM outperforms ADMM and ESTO in achieving higher spectral efficiency. This trend continues across spectral efficiency per cell, total efficiency, optimal scheduling of UEs, and the optimal number of users. The findings underscore the advanced optimization capabilities of HC-ADMM in various aspects of base station tower operations. The comprehensive superiority of HC-ADMM in spectral efficiency, efficiency per cell, total efficiency, and user scheduling positions it as a promising approach for enhancing the overall performance of communication networks.

REFERENCES

- [1] U. D. Ulusar, F. Al-Turjman, and G. Celik, "An overview of internet of things and wireless communications," in *2017 International Conference on Computer Science and Engineering (UBMK)*, IEEE, Oct. 2017, pp. 506–509. doi: 10.1109/UBMK.2017.8093446.
- [2] S. A. Dehkordi, K. Farajzadeh, J. Rezaezadeh, R. Farahbakhsh, K. Sandrasegaran, and M. A. Dehkordi, "A survey on data aggregation techniques in IoT sensor networks," *Wireless Networks*, vol. 26, no. 2, pp. 1243–1263, Feb. 2020, doi: 10.1007/s11276-019-02142-z.
- [3] B. Yin and X. Wei, "Communication-efficient data aggregation tree construction for complex queries in iot applications," *IEEE Internet of Things Journal*, vol. 6, no. 2, pp. 3352–3363, Apr. 2019, doi: 10.1109/JIOT.2018.2882820.
- [4] X. Lu, J. Liu, and H. Zhao, "Collaborative target tracking of IoT heterogeneous nodes," *Measurement*, vol. 147, p. 106872, Dec. 2019, doi: 10.1016/j.measurement.2019.106872.
- [5] C. Jiang, J. Xie, J. Zhao, and X. Zhang, "A novel high-voltage transmission line joint temperature monitoring system using hybrid communication networks," *IEEE Access*, vol. 9, pp. 109478–109487, 2021, doi: 10.1109/ACCESS.2021.3097372.
- [6] S. Gong, S. Ma, C. Xing, and G. Yang, "Optimal beamforming and time allocation for partially wireless powered sensor networks with downlink SWIPT," *IEEE Transactions on Signal Processing*, vol. 67, no. 12, pp. 3197–3212, Jun. 2019, doi: 10.1109/TSP.2019.2912876.
- [7] D. B. Rawat, T. White, M. S. Parwez, C. Bajracharya, and M. Song, "Evaluating secrecy outage of physical layer security in large-scale MIMO wireless communications for cyber-physical systems," *IEEE Internet of Things Journal*, vol. 4, no. 6, pp. 1987–1993, Dec. 2017, doi: 10.1109/JIOT.2017.2691352.
- [8] W. Feng, J. Wang, Y. Chen, X. Wang, N. Ge, and J. Lu, "UAV-aided MIMO communications for 5G internet of things," *IEEE Internet of Things Journal*, vol. 6, no. 2, pp. 1731–1740, Apr. 2019, doi: 10.1109/JIOT.2018.2874531.
- [9] S. Gong, C. Xing, S. Chen, and Z. Fei, "Secure communications for dual-polarized MIMO systems," *IEEE Transactions on Signal Processing*, vol. 65, no. 16, pp. 4177–4192, Aug. 2017, doi: 10.1109/TSP.2017.2706180.
- [10] S. Gong, S. Wang, S. Chen, C. Xing, and X. Wei, "Time-invariant joint transmit and receive beam pattern optimization for polarization-subarray based frequency diverse array radar," *IEEE Transactions on Signal Processing*, vol. 66, no. 20, pp. 5364–5379, Oct. 2018, doi: 10.1109/TSP.2018.2868041.
- [11] B. Wang, F. Gao, S. Jin, H. Lin, and G. Y. Li, "Spatial-and frequency-wideband effects in millimeter-wave massive MIMO systems," *IEEE Transactions on Signal Processing*, vol. 66, no. 13, pp. 3393–3406, Jul. 2018, doi: 10.1109/TSP.2018.2831628.
- [12] Y. Liu and J. Li, "Linear precoding to optimize throughput, power consumption and energy efficiency in MIMO wireless sensor networks," *IEEE Transactions on Communications*, vol. 66, no. 5, pp. 2122–2136, May 2018, doi: 10.1109/TCOMM.2018.2794363.
- [13] N. K. D. Venkatesowda, B. B. Narayana, and A. K. Jagannatham, "Precoding for robust decentralized estimation in coherent-MAC-based wireless sensor networks," *IEEE Signal Processing Letters*, vol. 24, no. 2, pp. 240–244, Feb. 2017, doi: 10.1109/LSP.2017.2647984.
- [14] S. Domouchtsidis, C. G. Tsinos, S. Chatzinotas, and B. Ottersten, "Symbol-level precoding for low complexity transmitter architectures in large-scale antenna array systems," *IEEE Transactions on Wireless Communications*, vol. 18, no. 2, pp. 852–863, Feb. 2019, doi: 10.1109/TWC.2018.2885525.
- [15] A. F. Molisch *et al.*, "Hybrid beamforming for massive MIMO: a survey," *IEEE Communications Magazine*, vol. 55, no. 9, pp. 134–141, 2017, doi: 10.1109/MCOM.2017.1600400.
- [16] F. Sohrabi and W. Yu, "Hybrid analog and digital beamforming for mmWave OFDM large-scale antenna arrays," *IEEE Journal on Selected Areas in Communications*, vol. 35, no. 7, pp. 1432–1443, Jul. 2017, doi: 10.1109/JSAC.2017.2698958.
- [17] H. Liu, S. Wang, X. Zhao, S. Gong, N. Zhao, and T. Q. S. Quek, "Analog-digital hybrid transceiver optimization for data aggregation in IoT networks," *IEEE Internet of Things Journal*, vol. 7, no. 11, pp. 11262–11275, Nov. 2020, doi: 10.1109/JIOT.2020.2996744.
- [18] C. G. Tsinos, S. Maleki, S. Chatzinotas, and B. Ottersten, "On the energy-efficiency of hybrid analog-digital transceivers for single- and multi-carrier large antenna array systems," *IEEE Journal on Selected Areas in Communications*, vol. 35, no. 9, pp. 1980–1995, Sep. 2017, doi: 10.1109/JSAC.2017.2720918.
- [19] R. Zhang, J. Zhou, J. Lan, B. Yang, and Z. Yu, "A high-precision hybrid analog and digital beamforming transceiver system for 5G millimeter-wave communication," *IEEE Access*, vol. 7, pp. 83012–83023, 2019, doi: 10.1109/ACCESS.2019.2923836.
- [20] L. Zhao, M. Li, C. Liu, S. V. Hanly, I. B. Collings, and P. A. Whiting, "Energy efficient hybrid beamforming for multi-user millimeter wave communication with low-resolution A/D at transceivers," *IEEE Journal on Selected Areas in Communications*, vol. 38, no. 9, pp. 2142–2155, Sep. 2020, doi: 10.1109/JSAC.2020.3000880.
- [21] M. Darabi, A. C. Cirik, and L. Lampe, "Transceiver design in millimeter wave full-duplex multi-user massive MIMO communication systems," *IEEE Access*, vol. 9, pp. 165394–165408, 2021, doi: 10.1109/ACCESS.2021.3135758.
- [22] S. He, J. Wang, Y. Huang, B. Ottersten, and W. Hong, "Codebook-based hybrid precoding for millimeter wave multiuser systems," *IEEE Transactions on Signal Processing*, vol. 65, no. 20, pp. 5289–5304, Oct. 2017, doi: 10.1109/TSP.2017.2723353.
- [23] A. W. Shaban, O. Damen, Y. Xin, and E. Au, "statistically-aided codebook-based hybrid precoding for mmWave single-user MIMO systems," in *2020 IEEE International Conference on Communications Workshops (ICC Workshops)*, IEEE, Jun. 2020, pp. 1–6. doi: 10.1109/ICCWorkshops49005.2020.9145199.
- [24] W. Ni, X. Dong, and W.-S. Lu, "Near-optimal hybrid processing for massive MIMO systems via matrix decomposition," *IEEE Transactions on Signal Processing*, vol. 65, no. 15, pp. 3922–3933, Aug. 2017, doi: 10.1109/TSP.2017.2699643.
- [25] G. Zhu, H. Huang, V. K. N. Lau, B. Xia, X. Li, and S. Zhang, "Hybrid beamforming via the kronecker decomposition for the millimeter-wave massive MIMO systems," *IEEE Journal on Selected Areas in Communications*, vol. 35, no. 9, pp. 2097–2114, Sep. 2017, doi: 10.1109/JSAC.2017.2720099.
- [26] X. Qiao, Y. Zhang, M. Zhou, and L. Yang, "Alternating optimization based hybrid precoding strategies for millimeter wave MIMO systems," *IEEE Access*, vol. 8, pp. 113078–113089, 2020, doi: 10.1109/ACCESS.2020.3002788.
- [27] J. Liu, H. Deng, S. Wang, G. Liu, K. Yang, and Z. Zhu, "Initial value acceleration-based alternating minimization algorithm for dynamic sub-connected hybrid precoding in millimeter wave MIMO systems," *Symmetry*, vol. 13, no. 2, p. 248, Feb. 2021, doi: 10.3390/sym13020248.
- [28] C. Xing, X. Zhao, W. Xu, X. Dong, and G. Y. Li, "A framework on hybrid MIMO transceiver design based on matrix-monotonic optimization," *IEEE Transactions on Signal Processing*, vol. 67, no. 13, pp. 3531–3546, Jul. 2019, doi: 10.1109/TSP.2019.2912833.

- [29] C. G. Tsinos, S. Chatzinotas, and B. Ottersten, "Hybrid analog-digital transceiver designs for multi-user MIMO mmWave cognitive radio systems," *IEEE Transactions on Cognitive Communications and Networking*, vol. 6, no. 1, pp. 310–324, Mar. 2020, doi: 10.1109/TCCN.2019.2933423.
- [30] C. G. Tsinos and B. Ottersten, "An efficient algorithm for unit-modulus quadratic programs with application in beamforming for wireless sensor networks," *IEEE Signal Processing Letters*, vol. 25, no. 2, pp. 169–173, Feb. 2018, doi: 10.1109/LSP.2017.2779276.
- [31] P. Huang, Y. Hao, T. Lv, J. Xing, J. Yang, and P. T. Mathiopoulos, "Secure beamforming design in relay-assisted internet of things," *IEEE Internet of Things Journal*, vol. 6, no. 4, pp. 6453–6464, Aug. 2019, doi: 10.1109/JIOT.2019.2908821.
- [32] H. Guo, Z. Yang, Y. Zou, T. Tsiftsis, M. R. Bhatangar, and R. C. De Lamare, "Secure beamforming for cooperative wireless-powered networks with partial CSI," *IEEE Internet of Things Journal*, vol. 6, no. 4, pp. 6760–6773, Aug. 2019, doi: 10.1109/JIOT.2019.2911356.
- [33] Z. Xiao, H. Dong, L. Bai, D. O. Wu, and X.-G. Xia, "Unmanned aerial vehicle base station (UAV-BS) deployment with millimeter-wave beamforming," *IEEE Internet of Things Journal*, vol. 7, no. 2, pp. 1336–1349, Feb. 2020, doi: 10.1109/JIOT.2019.2954620.
- [34] F. Yang, G. Pei, L. Hu, L. Ding, and Y. Li, "Joint optimization of SINR and maximum sidelobe level for hybrid beamforming systems with sub-connected structure," *Digital Signal Processing*, vol. 109, p. 102917, Feb. 2021, doi: 10.1016/j.dsp.2020.102917.
- [35] J. Deng, H. Li, J. A. Zhang, X. Huang, and Z. Cheng, "Transceiver optimization for mm wave line-of-sight MIMO systems using hybrid arrays," *Micromachines*, vol. 14, no. 2, p. 236, Jan. 2023, doi: 10.3390/mi14020236.

BIOGRAPHIES OF AUTHORS



Mrs. Jyothi B. R.    received the B.E. Degree in Electronics and Communication stream and M. Tech degree in VLSI and Embedded Systems from VTU, Belagavi in 2008 and 2014. She is pursuing Ph.D. degree in VTU, Belagavi, and serving as an Assistant Professor in ECE Department, KLS's Gogte Institute of Technology, Belagavi. Her research interests are in the area of signal processing, wireless sensor networks, communication networks, and IoT. She can be contacted at email: jyothiresearch2024@gmail.com.



Dr. Manjanaik Naganaik    Professor, Department of Electronics and Communication Engineering, University B.D.T College of Engineering, Davanagere, Karnataka, India. Graduated from University B.D.T College of Engineering, Davanagere. Kuvempu University, Shivamogga. A constituent College of VTU Belagavi. Has 22 years of Experience in teaching. He completed Ph. D, from Jain University, Bengaluru, He served various positions BOS, BOE Member at Visveswaraya Technological University. Published more than 15 Journals and Guided more than 25 PG Students, presently guiding 05 Ph.D, students and 01 student is already awarded. Interested areas are image and video processing, signal processing, and pattern recognition. He can be contacted at email: manjubdt2009@gmail.com.